



Potassium ion pre-intercalated MnO₂ for aqueous multivalent ion batteries

Zikang Xu¹ · Ruiqi Ren¹ · Hang Ren¹ · Jingyuan Zhang¹ · Jinyao Yang¹ · Jiawen Qiu¹ · Yizhou Zhang¹ · Guoyin Zhu¹ · Liang Huang² · Shengyang Dong¹

Received: 17 August 2023 / Accepted: 6 October 2023
© The Author(s) 2023

Abstract

Manganese dioxide (MnO₂), as a cathode material for multivalent ion (such as Mg²⁺ and Al³⁺) storage, is investigated due to its high initial capacity. However, during multivalent ion insertion/extraction, the crystal structure of MnO₂ partially collapses, leading to fast capacity decay in few charge/discharge cycles. Here, through pre-intercalating potassium-ion (K⁺) into δ-MnO₂, we synthesize a potassium ion pre-intercalated MnO₂, K_{0.21}MnO₂·0.31H₂O (KMO), as a reliable cathode material for multivalent ion batteries. The as-prepared KMO exhibits a high reversible capacity of 185 mAh/g at 1 A/g, with considerable rate performance and improved cycling stability in 1 mol/L MgSO₄ electrolyte. In addition, we observe that aluminum-ion (Al³⁺) can also insert into a KMO cathode. This work provides a valid method for modification of manganese-based oxides for aqueous multivalent ion batteries.

Keywords Aqueous batteries · Multivalent ion batteries · Magnesium ion · Aluminum ion · MnO₂

1 Introduction

Li-ion batteries (LIBs) have penetrated all aspects of the society, in portable electronics, electric mobility equipment, and even in large-scale energy storage systems [1–5]. Unluckily, with the shortage of lithium resources, the utilization of LIBs will be hindered by the rising price in the future. This problem has stimulated the investigation of promising alternatives. Due to the merits of low cost, low installation requirements, and high-level safety, aqueous rechargeable batteries (ARBs) offer an ideal option for dealing with future

energy-demand pressure [6–9]. While relatively low energy density is one of the main issues of ARBs [10–12], pairing multivalent ion carriers and exploiting high capacity cathode materials provide effective strategies to conquer the problem [13–16]. Unlike mono-valent carriers, such as Na⁺ and K⁺, multivalent cations have the ability to transfer more than one electron, and thereby to potentially provide better energy storage. To date, ARBs based on multivalent cations, for example Zn²⁺, Mg²⁺, Ca²⁺, and Al³⁺, have received a lot of attention [17–20]. In particular, various effective strategies have been put forward to optimize the electrochemical behavior of Zn²⁺ storage. These approaches include the perfection of cathode materials, such as porous and tunable MOFs [21], and anode modifications [22]. Very recently, Zhou's group proposed in situ preparation of a multi-layer electro-cross-linked electrolyte [23]. Based on such electrolyte, the assembled Zn/Zn–Alg-5/MnO₂ full cell not only provides outstanding electrochemical performances but offers potential for practical application. However, the field of aqueous magnesium-ion batteries (MIBs) still suffers from inadequate research despite the batteries' unique advantages.

Mg is the fifth most abundant metal element in the Earth's crust [24–26], making it a cost-effective material for scale application. However, sluggish kinetics of divalent ions in

✉ Guoyin Zhu
gyzhu@nuist.edu.cn

✉ Liang Huang
huangliang421@hust.edu.cn

✉ Shengyang Dong
dongsynt@nuist.edu.cn

¹ School of Environmental Science and Engineering, School of Chemistry and Materials Science, Nanjing University of Information Science and Technology, Nanjing 210044, China

² Wuhan National Laboratory for Optoelectronics, School of Optical and Electronic Information, Huazhong University of Science and Technology, Wuhan 430074, China

electrode materials, caused by strong electrostatic interactions between Mg^{2+} and anions in a host framework, induces a high overpotential and a low degree of magnesianation [27, 28]. In recent years, Chevrel phase Mo_6S_8 [29], MnO_2 [30] and layered V_2O_5 [31] have been explored for Mg^{2+} storage. Among these candidates, MnO_2 has received a lot of attention due to its high theoretical capacity, readily accessible, low cost and environmental compatibility [32]. Up to date, variant phases of MnO_2 , including hollandite $\alpha\text{-MnO}_2$ [33, 34], spinel $\lambda\text{-MnO}_2$ [35], and birnessite $\delta\text{-MnO}_2$ [36], have been studied and the research has obtained remarkable progress.

Nevertheless, serious capacity decay of MnO_2 cycling in aqueous electrolytes is frequently observed. In recent years, employing a pre-intercalation strategy to enhance electrochemical behavior and stabilize structure integrity has been proven to be an effective method [37]. As reported by Mai's group, the structural stability of layered vanadium oxide for Mg^{2+} storage can be improved through alkali ion pre-intercalating [38]. Thus, modifying the structure of MnO_2 to realize more stable insertion/extraction of Mg^{2+} and obtain considerable reversible capacity is an urgent priority.

Herein, we report a potassium ion (K^+) pre-intercalated $\text{K}_{0.21}\text{MnO}_2 \cdot 0.31\text{H}_2\text{O}$ (KMO) as a cathode material for Mg^{2+} hosting. Through a simple sol-gel process, K^+ is pre-intercalated into $\delta\text{-MnO}_2$, and the layered framework is stabilized,

realizing reversible insertion/extraction of Mg^{2+} . The KMO cathode in this study delivered a high specific capacity of 163 mAh/g at 0.1 A/g, satisfying rate performance, and improved long-term cycling stability. Additionally, KMO exhibits capability of aluminum ion (Al^{3+}) storage, implying potential application in aqueous aluminum-ion batteries (AIBs) even though further modifications are still required.

2 Results and discussion

The crystalline structure of KMO was firstly characterized by powder X-ray diffraction (XRD). As displayed in Fig. 1a, the diffraction pattern shows the diffraction peaks of $\text{K}_{0.27}\text{MnO}_2 \cdot 0.54\text{H}_2\text{O}$ (JCPDS No. 86-0666), which builds up by layers of edge-shared MnO_6 (Fig. 1b). The scanning electron microscopy (SEM) image (in Fig. 1c) demonstrate that KMO possesses a nanoparticle morphology with a size of 50–100 nm. The elemental energy-dispersive X-ray (EDX) spectroscopy mapping using SEM shows that the distribution of various elements including K, Mn, and O are uniform (Fig. 1d). Besides, according to the elemental mapping, the atomic ratio of K and Mn in KMO is about 0.23 (Table S1). The morphology of nanoparticles can be further revealed by transmission electron microscopy (TEM) imagery (Fig. 1e). Meanwhile, the interplanar distance of 0.71 nm (Fig. 1f)

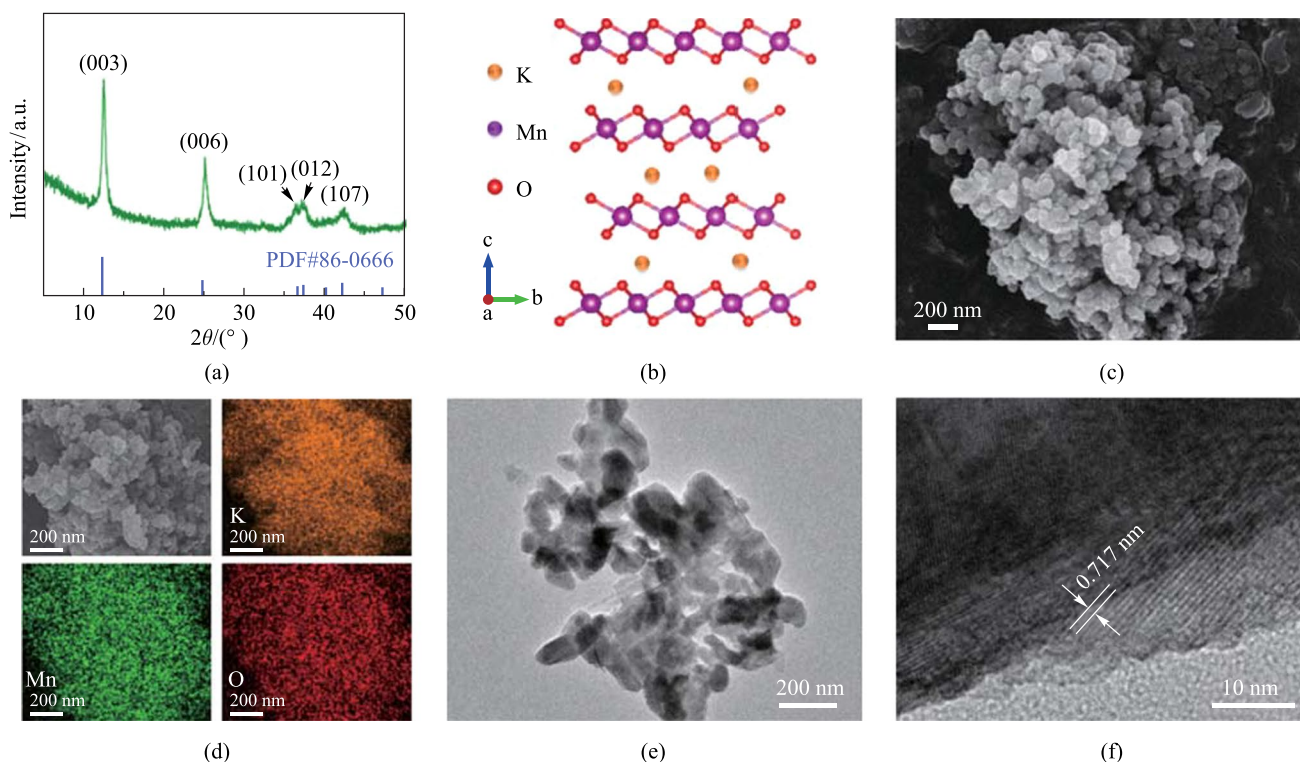


Fig. 1 Structural characterizations of KMO. **a** XRD pattern. **b** Crystal structure schematic of KMO. **c** SEM image. **d** Elemental mapping. **e**, **f** TEM images

demonstrates the (003) crystal plane of KMO. According to the data of inductively coupled plasma optical emission spectrometer (ICP-OES; can be found in Table S2) and thermogravimetric (TG) analysis (Fig. S1), the speculated formula of the as-prepared KMO is $K_{0.21}MnO_2 \cdot 0.31H_2O$.

The electrochemical performances of KMO were evaluated in three-electrode cells, with the potential window limited from -0.2 to 1.1 V, and 1 mol/L $MgSO_4$ solution as the electrolyte (All potentials below are relative to those for Ag/AgCl). As shown in Fig. 2a, the cyclic voltammetry (CV) curves almost overlap after the first cycle, which hints at the high electrochemical reversibility of KMO regarding magnesium ion storage. Notably, in the first five galvanostatic charge–discharge (GCD) profiles (Fig. 2b), KMO electrode provides approximately 163 mAh/g charge capacity at the current density of 0.1 A/g without obvious capacity degradation. In addition, when raising the current density from 0.1 to 10 A/g, the electrode exhibits a benign rate performance with approximately 78 mAh/g at 10 A/g. It is worth noting that the capacity slightly improves, compared to that of the initial value at 0.1 A/g, when the current density returns to 0.1 A/g again, which may arise from an activation process. Such a phenomenon also happened when carrying out the long-term cycling test, with the capacity increasing from 110 mAh/g to the highest capacity of 185 mAh/g at the high current density of 1 A/g.

What's more, the KMO delivered favorable cycling performance of Mg^{2+} storage, remaining about 86.7% capacity retention of the maximum over 1000 cycles, exceeding the majority of MnO_2 cathode materials that have been reported [27, 34, 39]. Further, electrochemical impedance spectroscopy (EIS) was conducted to check the activation process. Figure 2e shows that after 125 th and 250 th cycles, and relative to pristine, the KMO cathode shows a smaller semicircle in the high-frequency zone and a line with a larger slope in the low-frequency zone than initial, implying a smaller charge-transfer resistance and faster Mg^{2+} diffusion kinetics after the cycling process. Such results further prove the capacity increase and activation process during cycling.

Furthermore, a cyclic voltammetry (CV) test under different scan rates was carried out to evaluate the electrochemical kinetics of a KMO electrode for Mg^{2+} storage. As depicted in Fig. 3a, during the increase of scan rates, the reduction/oxidation peak currents become apparently increased, and the shapes of CV curves show good agreement, indicating the excellent electrochemical reversibility of the KMO electrode. Typically, the stored charge originates from two parts: diffusion-dominated process and non-diffusion-dominated capacitive process, and the capacity contribution can be calculated by the power-law equation [40]:

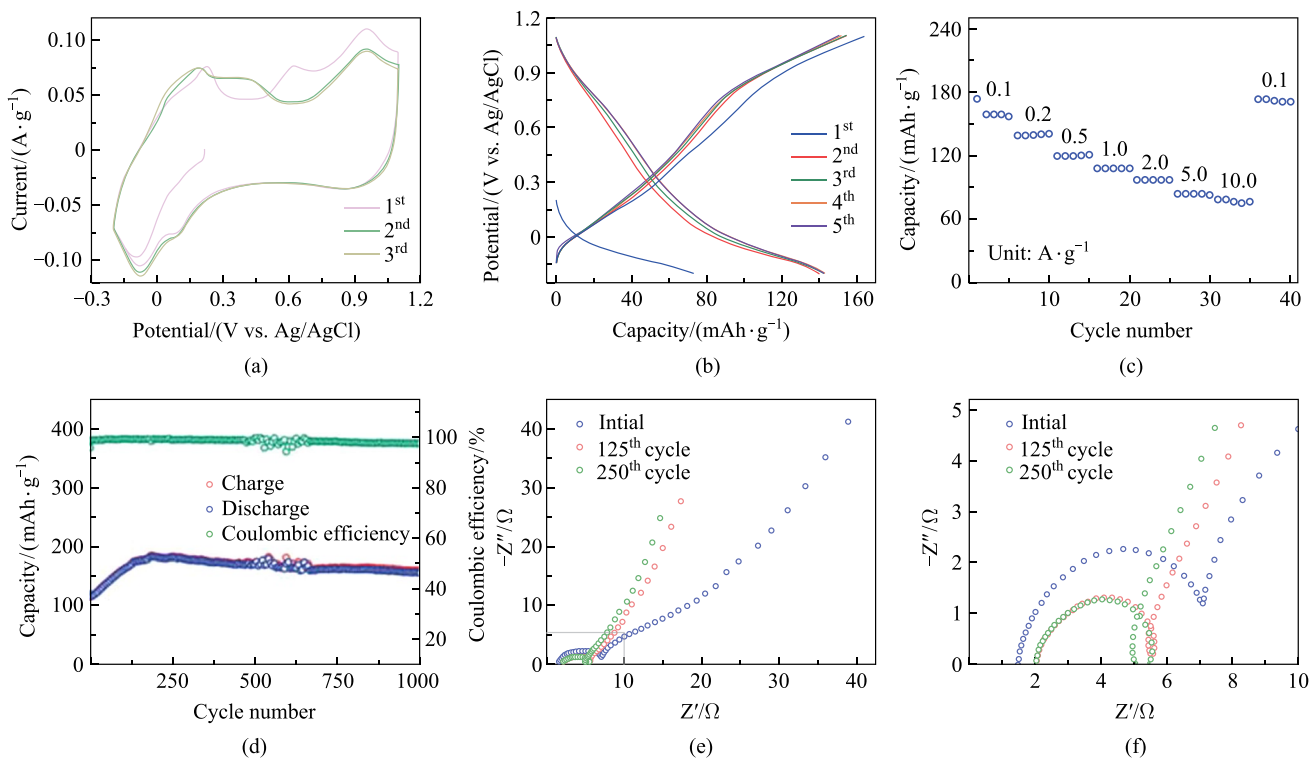


Fig. 2 Electrochemical behaviors of KMO. **a** CV profiles at 0.2 mV/s. **b** First five GCD curves at 0.1 A/g. **c** Rate performance from 0.1 to 10.0 A/g. **d** Long-term cycling stability at 1 A/g. **e**, **f** EIS plots at different cycles

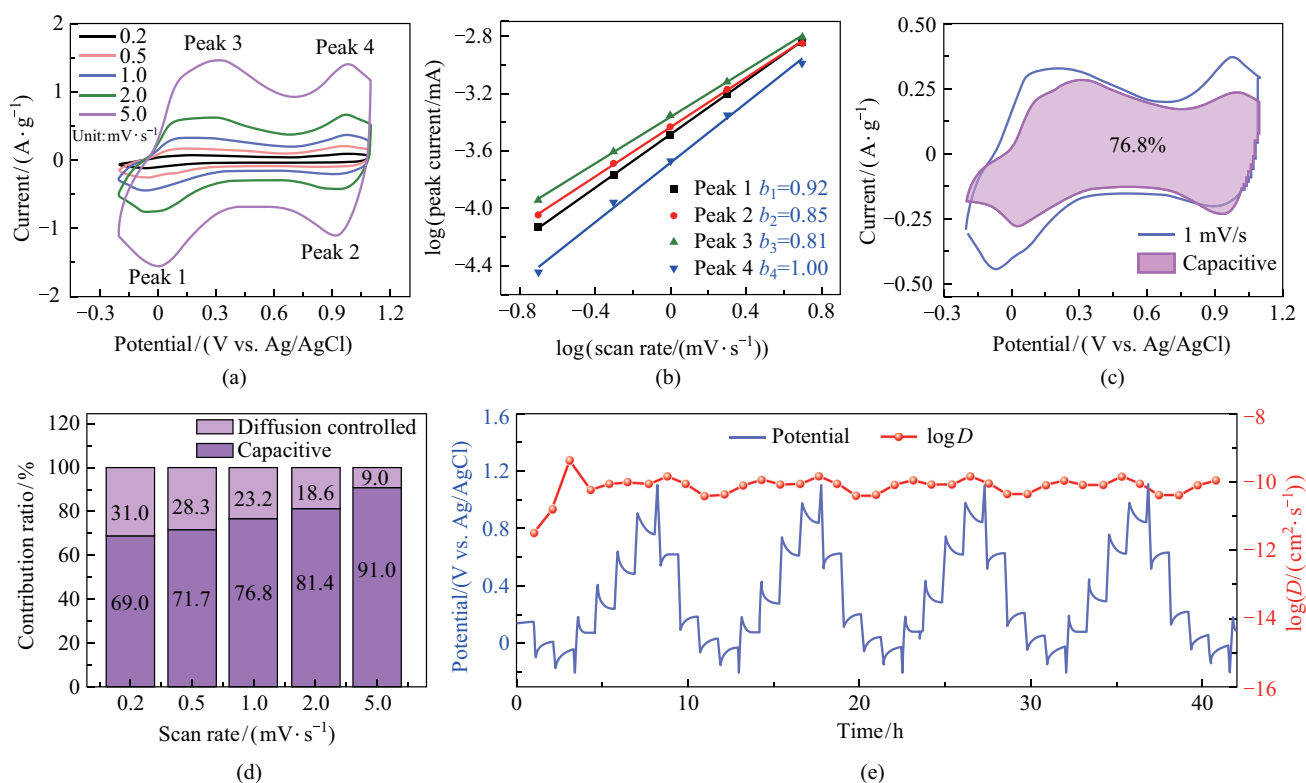


Fig. 3 Kinetic analysis of KMO electrode. **a** CV curves at different scan rates. **b** $\log(i)$ vs. $\log(v)$ plots of reduction/oxidation currents response. **c** Capacitive contribution at 1 mV/s. **d** Contribution ratio of diffusion-dominated capacities and non-diffusion-dominated capacities at different scan rates. **e** GCD profiles with the GITT test (0.1 A/g for 10 min and then 1 h rest) and the corresponding diffusion coefficient

$$i = av^b, \quad (1)$$

where i represents the peak currents, a and b represent coefficients, and v signals the scan rate. Additionally, the b value is used to assess the capacity domination. When b is 0.5, the capacity is determined by the diffusion-controlled behavior, while $b = 1$ indicates the capacitive process.

Equation (1) can be further transformed to the formulation:

$$\log(i) = \log(a) + b\log(v). \quad (2)$$

Thus, the values of b can be calculated from the slopes of $\log(i)$ vs. $\log(v)$. Moreover, the specific contribution of the two processes can be calculated through Eq. (3) [41]:

$$i = k_1v + k_2v^{1/2}, \quad (3)$$

where k_1v represents the capacitive-type contribution, while $k_2v^{1/2}$ denotes the diffusion-controlled counterpart. As shown in Fig. 3b, the b values vary from 0.8 to 1, indicating that the capacity is controlled by a combination of the both of the processes. Meanwhile, the contribution of capacitive-controlled storage gradually increases when increasing the

scan rates from 0.2 to 5 mV/s, and the proportion of capacitive storage finally comes to 91% at 5 mV/s (Fig. 3c, d and Fig. S2). To further evaluate the diffusion kinetics of Mg^{2+} in the KMO electrode, the galvanostatic intermittent titration technique (GITT) was implemented. The result, presented in Fig. 3e, shows that the calculated diffusion coefficient is between 10^{-10} and 10^{-9} cm^2/s , indicating fast Mg^{2+} conduction in KMO [42–45].

Ex-situ XRD was conducted to investigate the structure evolution of KMO during the Mg^{2+} storage process. The first cycle of the GCD profile and corresponding XRD patterns are described in Fig. S3a and S3b. No new diffraction peaks are detected during insertion/extraction of Mg^{2+} , demonstrating that KMO maintains a consistent layered structure. As displayed, the (003) peak (enlarged in Fig. S3c) shifts slightly to a higher 2θ angles during the discharge process, suggesting the decrease of the corresponding interlayer spacing. After a full charge/discharge cycle, the behavior of the (003) plane shows subtle deviation, demonstrating a reversible insertion/extraction of Mg^{2+} . According to the data of ICP-OES, shown in Table S3, the content of Mg^{2+} in the electrolyte increases from the first uncharged to charged

state, implying the existence of Mg^{2+} extraction from electrode. Meanwhile, the concentration of K^+ slightly increases, which may arise from minor co-extraction of K^+ along with Mg^{2+} . In addition, the dissolution problem of manganese in MnO_2 can be effectively inhibited.

We also compared the electrochemical behaviors of the KMO in 1 mol/L ZnSO_4 aqueous electrolyte. As shown in Fig. S4a, a couple of redox peaks at around 0.42 and 0.58 V can be found at 1 mV/s. Fast capacity loss and unfavorable rate capability also happened for Zn^{2+} storage (Fig. S4b and S4c). For example, only 37.2 mAh/g could be retained at 2 A/g. Besides, KMO suffers a fast capacity loss in the initial cycles (Fig. S4d).

We selected VO_2 (Fig. S5a, monoclinic VO_2 (B) phase) as an anode and fabricated a full cell with a KMO cathode. Briefly, a VO_2 anode could provide a reversible capacity of about 150 mAh/g at a current density of 0.1 A/g (Fig. S5b). As shown in Fig. S5c, when the current density was increased to 1 A/g, the capacity of 41.1 mAh/g could be retained. A capacity retention of 80.9% could be obtained after 300 cycles at 1 A/g. The assembled $\text{KMO}||\text{VO}_2$ full cell could deliver about 80 mAh/g based on the active mass of

cathode at 0.1 A/g (Fig. S6a). When the current density was elevated to 1 A/g, the corresponding capacity was about 20 mAh/g (Figure S6b). Besides, the capacity retention was about 58.0% after 100 cycles.

Since divalent Mg^{2+} can effectively insert into the KMO electrode, we suspected that Al^{3+} can also insert into KMO. We conducted routine electrochemical measurements to test this. Figure 4a shows the first three CV curves with a pair of distinct redox peaks at around 0.80 and 0.93 V. Typically, from the first discharge profile in Fig. 4b, an obvious discharge plateau can be detected, which may result from the structure reconfiguration. As is well-acknowledged, the inserted Al^{3+} ions generally possess relatively high electrostatic interaction with the host materials, and thus causes structural collapse, leading to fast capacity decay and poor cycling stability [46–48]. Such a disadvantage applies to the KMO electrode as well, which can be detected from the GCD curves. After five cycles, the specific charge capacity quickly faded from 200 to 125 mAh/g. As shown in Fig. 4c, only 28.3 mAh/g could be obtained at 2 A/g. On the other hand, poor cycling capacity (capacity retention of 45.1% after 1000

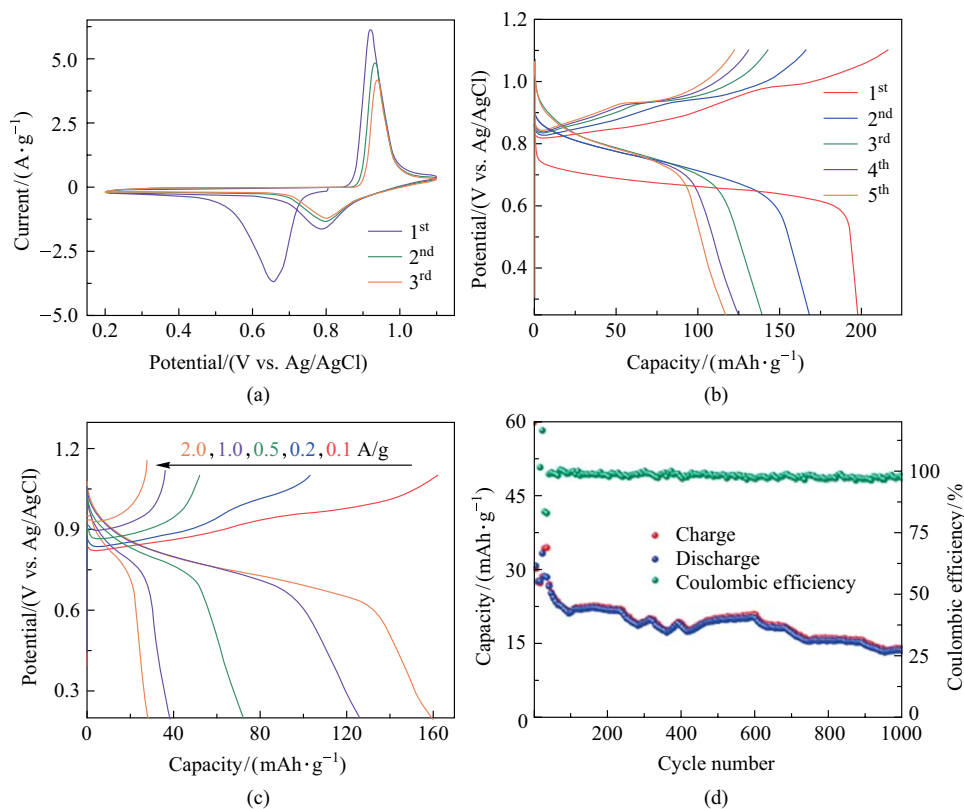


Fig. 4 Electrochemical performance of KMO electrode for Al^{3+} storage. **a** CV curves at 1 mV/s. **b** First five GCD curves at 0.1 A/g in 0.5 mol/L $\text{Al}_2(\text{SO}_4)_3$ electrolyte. **c** Rate performance. **d** Cycling stability at 0.5 A/g

cycles at 0.5 A/g) also creates a requirement for more in-depth modification of KMO structure. KMO has the ability to store Al^{3+} in aqueous electrolyte, but further investigation, for all potential electrode materials and electrolytes, is needed.

3 Conclusions

In summary, through pre-intercalating potassium ions into manganese dioxide, we explored an effective cathode material for Mg^{2+} storage. The KMO electrode can deliver a considerable capacity of 185 mAh/g at a current density of 1 A/g in 1 mol/L MgSO_4 aqueous solution. In addition, after an activation process, the electrochemical impedance greatly decreases and the layered-structure KMO material exhibits improved rate capability (78 mAh/g at a current density of 10 A/g) and long-term cycling stability (capacity retention 86.7% over 1000 cycles). Moreover, Al^{3+} can also be inserted into the KMO host, but the structure transforms during Al^{3+} insertion/extraction. Further investigation is required to improve electrochemical performance. Finally, we believe that this work promotes the study of cathode materials for $\text{Mg}^{2+}/\text{Al}^{3+}$ storage and offers an insight to modification of metal-oxide cathodes for non-monovalent storage.

Supplementary Information The online version contains supplementary material available at <https://doi.org/10.1007/s12200-023-00093-0>.

Acknowledgements This work was supported by the National Natural Science Foundation of China (Grant No. 52102264), the Leading Edge Technology of Jiangsu Province (BK20220009), and the Open Project Program of Wuhan National Laboratory for Optoelectronics (No. 2020WNLOKF011).

Author contributions ZX carried out experiments, analyzed the data and drafted the manuscript. RR, HR, JZ, JY, JQ and YZ analyzed the data. GZ and LH analyzed the data and approved the final manuscript. SD designed the project and polished the manuscript. All authors contributed to the writing and revision of this paper.

Availability of data and materials The data that support the findings of this study are available from the corresponding author, upon reasonable request.

Declarations

Competing interests The authors declare that they have no competing interests.

Open Access This article is licensed under a Creative Commons Attribution 4.0 International License, which permits use, sharing, adaptation, distribution and reproduction in any medium or format, as long as you give appropriate credit to the original author(s) and the source, provide a link to the Creative Commons licence, and indicate if changes were made. The images or other third party material in this article are included in the article's Creative Commons licence, unless indicated otherwise in a credit line to the material. If material is not included in

the article's Creative Commons licence and your intended use is not permitted by statutory regulation or exceeds the permitted use, you will need to obtain permission directly from the copyright holder. To view a copy of this licence, visit <http://creativecommons.org/licenses/by/4.0/>.

References

- Hu, S., Pillai, A.S., Liang, G., Pang, W.K., Wang, H., Li, Q., Guo, Z.: Li-rich layered oxides and their practical challenges: recent progress and perspectives. *Electrochem. Energy Rev.* **2**(2), 277–311 (2019)
- Shao-Horn, Y., Croguennec, L., Delmas, C., Nelson, E.C., O'Keefe, M.A.: Atomic resolution of lithium ions in LiCoO_2 . *Nat. Mater.* **2**(7), 464–467 (2003)
- Tarascon, J.M., Armand, M.: Issues and challenges facing rechargeable lithium batteries. *Nature* **414**(6861), 359–367 (2001)
- Whittingham, M.S.: Lithium batteries and cathode materials. *Chem. Rev.* **104**(10), 4271–4302 (2004)
- Dong, S., Wu, Y., Lv, N., Ren, R., Huang, L.: Porous sodium titanate nanofibers for high energy quasi-solid-state sodium-ion hybrid capacitors. *Rare Met.* **41**(7), 2453–2459 (2022)
- Kim, H., Hong, J., Park, K., Kim, H., Kim, S., Kang, K.: Aqueous rechargeable Li and Na ion batteries. *Chem. Rev.* **114**(23), 11788–11827 (2014)
- Posada, J.O.G., Rennie, A.J.R., Villar, S.P., Martins, V.L., Marinaccio, J., Barnes, A., Glover, C.F., Worsley, D.A., Hall, P.J.: Aqueous batteries as grid scale energy storage solutions. *Renewable Sustain. Energy Rev.* **68**, 1174–1182 (2017)
- Zhang, H., Liu, X., Li, H., Hasa, I., Passerini, S.: Challenges and strategies for high-energy aqueous electrolyte rechargeable batteries. *Angew. Chem. Int. Ed.* **60**(2), 598–616 (2021)
- Tong, Y., Zhang, T., Sun, Y., Wang, X., Wu, X.: $\text{Co}_3\text{O}_4/\text{NiMoO}_4$ composite electrode materials for flexible hybrid capacitors. *Front. Optoelectron.* **15**(1), 25 (2022)
- Chen, S., Zhang, M., Zou, P., Sun, B., Tao, S.: Historical development and novel concepts on electrolytes for aqueous rechargeable batteries. *Energy Environ. Sci.* **15**(5), 1805–1839 (2022)
- Dong, S., Shin, W., Jiang, H., Wu, X., Li, Z., Holoubek, J., Stickle, W.F., Key, B., Liu, C., Lu, J., Greaney, P.A., Zhang, X., Ji, X.: Ultra-fast NH_4^+ storage: strong H Bonding between NH_4^+ and Bi-layered V_2O_5 . *Chem.* **5**(6), 1537–1551 (2019)
- Dong, S., Wang, Y., Chen, C., Shen, L., Zhang, X.: Niobium tungsten oxide in a green water-in-salt electrolyte enables ultra-stable aqueous lithium-ion capacitors. *Nano-Micro Lett.* **12**(1), 168 (2020)
- Liang, G., Mo, F., Yang, Q., Huang, Z., Li, X., Wang, D., Liu, Z., Li, H., Zhang, Q., Zhi, C.: Commencing an acidic battery based on a copper anode with ultrafast proton-regulated kinetics and superior dendrite-free property. *Adv. Mater.* **31**(52), 1905873 (2019)
- Wang, H., Tan, R., Yang, Z., Feng, Y., Duan, X., Ma, J.: Stabilization perspective on metal anodes for aqueous batteries. *Adv. Energy Mater.* **11**(2), 2000962 (2021)
- Yang, D., Zhou, Y., Geng, H., Liu, C., Lu, B., Rui, X., Yan, Q.: Pathways towards high energy aqueous rechargeable batteries. *Coord. Chem. Rev.* **424**, 213521 (2020)
- Famprikis, T., Canepa, P., Dawson, J.A., Islam, M.S., Masquelier, C.: Fundamentals of inorganic solid-state electrolytes for batteries. *Nat. Mater.* **18**(12), 1278–1291 (2019)
- Chen, D., Tao, D., Ren, X., Wen, F., Li, T., Chen, Z., Cao, Y., Xu, F.: A molybdenum polysulfide in-situ generated from ammonium tetrathiomolybdate for high-capacity and high-power rechargeable magnesium battery cathodes. *ACS Nano* **16**(12), 20510–20520 (2022)

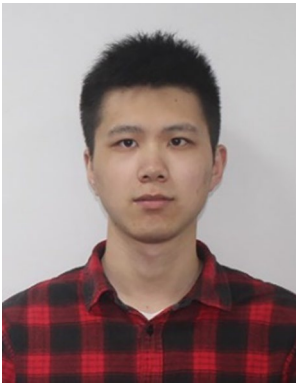
18. Liu, Y., Qin, Z., Yang, X., Liu, J., Liu, X.-X., Sun, X.: High-voltage manganese oxide cathode with two-electron transfer enabled by a phosphate proton reservoir for aqueous zinc batteries. *ACS Energy Lett.* **7**(5), 1814–1819 (2022)
19. Qin, X., Zhao, X., Zhang, G., Wei, Z., Li, L., Wang, X., Zhi, C., Li, H., Han, C., Li, B.: Highly reversible intercalation of calcium ions in layered vanadium compounds enabled by acetonitrile–water hybrid electrolyte. *ACS Nano* **17**(13), 12040–12051 (2023)
20. Yang, J., Gong, W., Geng, F.: Defect modulation in cobalt manganese oxide sheets for stable and high-energy aqueous aluminum-ion batteries. *Adv. Funct. Mater.* **33**(27), 2301202 (2023)
21. Peng, Z., Li, Y., Ruan, P., He, Z., Dai, L., Liu, S., Wang, L., Chan Jun, S., Lu, B., Zhou, J.: Metal-organic frameworks and beyond: the road toward zinc-based batteries. *Coord. Chem. Rev.* **488**, 215190 (2023)
22. Yi, R., Shi, X., Tang, Y., Yang, Y., Zhou, P., Lu, B., Zhou, J.: Carboxymethyl chitosan-modified zinc anode for high-performance zinc–iodine battery with narrow operating voltage. *Small Struct.* **4**(9), 2300020 (2023)
23. Xie, X., Li, J., Xing, Z., Lu, B., Liang, S., Zhou, J.: Biocompatible zinc battery with programmable electro-cross-linked electrolyte. *Natl. Sci. Rev.* **10**(3), nwac281 (2023)
24. You, C., Wu, X., Yuan, X., Chen, Y., Liu, L., Zhu, Y., Fu, L., Wu, Y., Guo, Y.-G., van Ree, T.: Advances in rechargeable Mg batteries. *J. Mater. Chem. A* **8**(48), 25601–25625 (2020)
25. Zhang, J., Chang, Z., Zhang, Z., Du, A., Dong, S., Li, Z., Li, G., Cui, G.: Current design strategies for rechargeable magnesium-based batteries. *ACS Nano* **15**(10), 15594–15624 (2021)
26. Pei, C., Xiong, F., Yin, Y., Liu, Z., Tang, H., Sun, R., An, Q., Mai, L.: Recent progress and challenges in the optimization of electrode materials for rechargeable magnesium batteries. *Small* **17**(3), 2004108 (2021)
27. Song, J., Noked, M., Gillette, E., Duay, J., Rubloff, G., Lee, S.B.: Activation of a MnO₂ cathode by water-stimulated Mg²⁺ insertion for a magnesium ion battery. *Phys. Chem. Chem. Phys.* **17**(7), 5256–5264 (2015)
28. Nam, K.W., Kim, S., Lee, S., Salama, M., Shterenberg, I., Gofer, Y., Kim, J.S., Yang, E., Park, C.S., Kim, J.S., Lee, S.S., Chang, W.S., Doo, S.G., Jo, Y.N., Jung, Y., Aurbach, D., Choi, J.W.: The high performance of crystal water containing manganese birnessite cathodes for magnesium batteries. *Nano Lett.* **15**(6), 4071–4079 (2015)
29. Saha, P., Jampani, P.H., Datta, M.K., Hong, D., Gattu, B., Patel, P., Kadakia, K.S., Manivannan, A., Kumta, P.N.: A rapid solid-state synthesis of electrochemically active Chevrel phases (Mo₆T₈; T = S, Se) for rechargeable magnesium batteries. *Nano Res.* **10**(12), 4415–4435 (2017)
30. Canepa, P., Sai Gautam, G., Hannah, D.C., Malik, R., Liu, M., Gallagher, K.G., Persson, K.A., Ceder, G.: Odyssey of multivalent cathode materials: open questions and future challenges. *Chem. Rev.* **117**(5), 4287–4341 (2017)
31. Andrews, J.L., Mukherjee, A., Yoo, H.D., Parija, A., Marley, P.M., Fakra, S., Prendergast, D., Cabana, J., Klie, R.F., Banerjee, S.: Reversible Mg-ion insertion in a metastable one-dimensional polymorph of V₂O₅. *Chem.* **4**(3), 564–585 (2018)
32. Augustyn, V., Simon, P., Dunn, B.: Pseudocapacitive oxide materials for high-rate electrochemical energy storage. *Energy Environ. Sci.* **7**(5), 1597–1614 (2014)
33. Zhang, R., Yu, X., Nam, K.-W., Ling, C., Arthur, T.S., Song, W., Knapp, A.M., Ehrlich, S.N., Yang, X.-Q., Matsui, M.: α -MnO₂ as a cathode material for rechargeable Mg batteries. *Electrochem. Commun.* **23**, 110–113 (2012)
34. Kim, J.-S., Chang, W., Kim, R., Kim, D., Han, D., Lee, K., Lee, S., Doo, S.: High-capacity nanostructured manganese dioxide cathode for rechargeable magnesium ion batteries. *J. Power. Sources* **273**, 210–215 (2015)
35. Chen, W., Zhan, X., Luo, B., Ou, Z., Shih, P., Yao, L., Pidaparthy, S., Patra, A., An, H., Braun, P.V., Stephens, R.M., Yang, H., Zuo, J., Chen, Q.: Effects of particle size on Mg²⁺ ion intercalation into λ -MnO₂ cathode materials. *Nano Lett.* **19**(7), 4712–4720 (2019)
36. Zhang, C., Zhan, X., Al-Zoubi, T., Ma, Y., Shih, P., Wang, F., Chen, W., Pidaparthy, S., Stephens, R.M., Chen, Q., Zuo, J., Yang, H.: Electrochemical generation of birnessite MnO₂ nanoflowers for intercalation of Mg²⁺ ions. *Nano Energy* **102**, 107696 (2022)
37. Clites, M., Pomerantseva, E.: Bilayered vanadium oxides by chemical pre-intercalation of alkali and alkali-earth ions as battery electrodes. *Energy Storage Mater.* **11**, 30–37 (2018)
38. Tang, H., Xiong, F., Jiang, Y., Pei, C., Tan, S., Yang, W., Li, M., An, Q., Mai, L.: Alkali ions pre-intercalated layered vanadium oxide nanowires for stable magnesium ions storage. *Nano Energy* **58**, 347–354 (2019)
39. Rasul, S., Suzuki, S., Yamaguchi, S., Miyayama, M.: High capacity positive electrodes for secondary Mg-ion batteries. *Electrochim. Acta* **82**, 243–249 (2012)
40. Augustyn, V., Come, J., Lowe, M.A., Kim, J.W., Taberna, P., Tolbert, S.H., Abruña, H.D., Simon, P., Dunn, B.: High-rate electrochemical energy storage through Li⁺ intercalation pseudocapacitance. *Nat. Mater.* **12**(6), 518–522 (2013)
41. Choi, C., Ashby, D.S., Butts, D.M., DeBlock, R.H., Wei, Q., Lau, J., Dunn, B.: Achieving high energy density and high power density with pseudocapacitive materials. *Nat. Rev. Mater.* **5**(1), 5–19 (2020)
42. Koketsu, T., Ma, J., Morgan, B.J., Body, M., Legein, C., Dachraoui, W., Giannini, M., Demortière, A., Salanne, M., Dardoize, F., Groult, H., Borkiewicz, O.J., Chapman, K.W., Strasser, P., Dambournet, D.: Reversible magnesium and aluminum ions insertion in cation-deficient anatase TiO₂. *Nat. Mater.* **16**(11), 1142–1148 (2017)
43. Wu, D., Zhuang, Y., Wang, F., Yang, Y., Zeng, J., Zhao, J.: High-rate performance magnesium batteries achieved by direct growth of honeycomb-like V₂O₅ electrodes with rich oxygen vacancies. *Nano Res.* **16**(4), 4880–4887 (2023)
44. Yuan, C., Zhang, Y., Pan, Y., Liu, X., Wang, G., Cao, D.: Investigation of the intercalation of polyvalent cations (Mg²⁺, Zn²⁺) into λ -MnO₂ for rechargeable aqueous battery. *Electrochim. Acta* **116**, 404–412 (2014)
45. Liu, M., Rong, Z., Malik, R., Canepa, P., Jain, A., Ceder, G., Persson, K.A.: Spinel compounds as multivalent battery cathodes: a systematic evaluation based on ab initio calculations. *Energy Environ. Sci.* **8**(3), 964–974 (2015)
46. Wu, C., Gu, S., Zhang, Q., Bai, Y., Li, M., Yuan, Y., Wang, H., Liu, X., Yuan, Y., Zhu, N., Wu, F., Li, H., Gu, L., Lu, J.: Electrochemically activated spinel manganese oxide for rechargeable aqueous aluminum battery. *Nat. Commun.* **10**(1), 73 (2019)
47. Gu, S., Wang, H., Wu, C., Bai, Y., Li, H., Wu, F.: Confirming reversible Al³⁺ storage mechanism through intercalation of Al³⁺ into V₂O₅ nanowires in a rechargeable aluminum battery. *Energy Storage Mater.* **6**, 9–17 (2017)
48. Yang, H., Li, H., Li, J., Sun, Z., He, K., Cheng, H.-M., Li, F.: The rechargeable aluminum battery: opportunities and challenges. *Angew. Chem. Int. Ed.* **58**(35), 11978–11996 (2019)



Zikang Xu received his bachelor's degree from Nanjing University of Information Science and Technology (NUIST), China. After that, he continued his postgraduate under the supervision of Prof. Shengyang Dong. His main research direction is aqueous electrochemical energy storage.



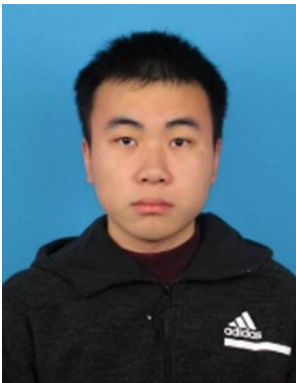
Jinyao Yang received his bachelor's degree in 2022 from the School of Materials Science and Engineering, Qilu University of Technology, China. And now, he is studying in Nanjing University of Information Science and Technology (NUIST), China under the supervision of Prof. Shengyang Dong. His main research direction is aqueous electrochemical energy storage, such as, NH_4 -ion batteries and Mg-ion batteries.



Ruiqi Ren is currently studying in Nanjing University of Information Science and Technology (NUIST), China under the supervision of Prof. Shengyang Dong. His main research direction is Li-ion batteries (LIBs).



Jiawen Qiu is currently studying in Nanjing University of Information Science and Technology (NUIST), China. His major is Materials Physics in School of Chemistry and Materials Science as an undergraduate.



Hang Ren obtained his bachelor's degree in 2022 from Shanghai University of Electric Power, China. Currently, he is studying at Nanjing University of Information Science and Technology (NUIST), China under the supervision of Prof. Shengyang Dong. His research primarily focuses on aqueous electrochemical energy storage.



Yizhou Zhang is a professor of Materials Science and Engineering at Nanjing University of Information Science and Technology (NUIST), China. He mainly works on functional materials for printed and flexible energy storage and electronics.



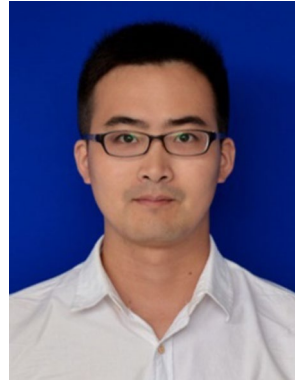
Jingyuan Zhang is currently studying in Nanjing University of Information Science and Technology (NUIST), China under the supervision of Prof. Shengyang Dong. His main research direction is dual-ion batteries, such as sodium-based dual-ion batteries and lithium-based dual-ion batteries.



Guoyin Zhu obtained his Ph.D. degree under the supervision of Prof. Zhong Jin at Nanjing University, China in 2018. Then, he joined Prof. Qing Chen's research group in The Hong Kong University of Science and Technology, China as a postdoctoral researcher. Now he works in Nanjing University of Information Science and Technology, China. His research focuses on the design, controllable preparation, energy storage mechanism of high-performance electrode materials and the application in energy storage technology.



Liang Huang is an associate professor in Wuhan National Laboratory for Optoelectronics (WNLO) at Huazhong University of Science and Technology (HUST), China. He received his Ph.D. degree from the Department of Chemistry and Chemical Engineering at Lanzhou University, China in 2013. He was a visiting student at North Carolina State University and Georgia Institute of Technology, USA in 2011–2013. His research interest is materials for energy conversion and storage.



Shengyang Dong received his Ph.D. degree in 2019 from Nanjing University of Aeronautics and Astronautics (NUAA), China, and then joined Nanjing University of Information Science and Technology (NUIST), China. From 2016 to 2017, he had studied at Oregon State University, USA as an exchange Ph.D. student. His research is now mainly focuses on the development of advanced materials for sustainable energy storage, such as aqueous batteries, hybrid capacitors, Na-ion batteries, and dual-ion batteries.